Proceedings of the
Annual Stability Conference
Structural Stability Research Council
Pittsburgh, Pennsylvania, May 10-14, 2011

Cyclic behavior and ductility evaluation of thin-walled stiffened steel box columns

I.H.P. Mamaghani[1], N. Nemati[2], E. Erdogan[2]

Abstract

This paper deals with cyclic behavior and ductility evaluation of thin-walled stiffened steel box columns subjected to cyclic lateral loading in the presence of constant axial load. The basic characteristics of steel box columns are noted. The results of finite-element analyses on cyclic elastoplastic behavior of steel box columns are presented. For comparison purposes, in the analysis three material models are employed for material nonlinearity to trace the inelastic cyclic behavior of steel: kinematic hardening, isotropic hardening, and elastic perfectly plastic. A method for evaluating ductility capacity of tubular columns is presented. The application of the method is demonstrated by comparing the computed strength and ductility of some cantilever columns with the test results.

1. Introduction

Thin-walled steel tubular bridge piers, with and without longitudinal and lateral stiffeners, in the form of cantilever columns and planar rigid frames, have been used in modern highway bridge systems because of their high strength and torsional rigidity. For example, Figure 1a shows bridge piers of thin-walled circular and rectangular box sections supporting an elevated highway bridge in Nagoya, Japan. These types of structures are susceptible to damage caused by local and overall interaction buckling when subjected to severe earthquakes because their sections are characterized by a large width-to-thickness ratio of the flange plate (for box section), and by a large radius-to-thickness ratio of the circular section. As is well known, a lot of steel piers buckled or collapsed during the Kobe earthquake (January 1995). Figure 1b shows an example of such a damaged pier.

[1] Associate Professor, Department of Civil Engineering, University of North Dakota, Grand Forks, ND, 58202-8115, USA. Email: irajmamaghani@mail.und.edu
[2]Formerly Graduate Student, Department of Civil Engineering University of North Dakota, 243 Centennial Dr., Grand Forks, ND, 58202-8115

(a) (b) (c)

Figure 1. (a) Thin-walled Steel Tubular Columns with Circular (Front) and Rectangular Box (Rare) Sections Supporting Elevated Highway Bridge in Nagoya, Japan, (b) Damaged Steel Bridge Pier During Kobe Earthquake (January 17, 1995), (c) Stiffened Box Section

To improve seismic capacity of steel bridge piers of tubular sections, a number of researchers, among others, Fukumoto (2004), Uenoya et al. (2003), Mamaghani (2008), Mamaghani et al. (2002, 1997, 1996, 1995), Hajjar (2000), Kitada et al. (2000), Nakanishi et al. (1999), Banno et al. (1998), Nishikawa et al. (1998, 1996), Gao et al. (1998), JRA(1996), Shen et al. (1995), and Usami et al. (1995) have experimentally and theoretically investigated the stability and plastic ductility of steel tubular columns. Based on the damage sustained by steel bridge piers in the Kobe earthquake and extensive test results, one of the important challanges of seismic design and retrofit of steel tubular columns is to increase the ductility of the columns while keeping their ultimate strength almost unchanged. Therefore a sound understanding of the cyclic inelastic behavior of thin-walled steel tubular columns is important in developing a rational performance-based seismic design methodology and ductility evaluation of such structures. Also seismic retrofits of existing steel tubular columns that do not satisfy the new seismic design method regulations are needed in order to enhance their strength and ductility.

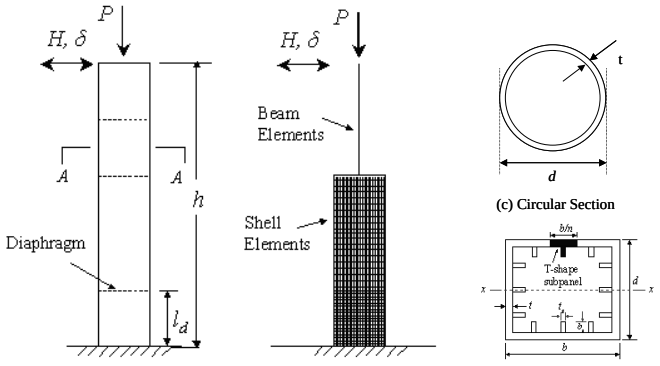

Figure 2. Modeling of Steel Tubular Columns: (a) Steel Tubular Column , (b) Analytical Model, (c) Circular Section, (d) Stiffened Rectangular Section

In this paper, the basic characteristics of thin-walled steel tubular columns are noted. The results of a finite-element analysis on cyclic elastoplastic behavior of steel tubular columns are presented. The isotropic hardening (IH), kinematic hardening (KH), and elastic perfectly plastic (EPP) material models are employed for material nonlinearity to trace the inelastic cyclic behavior of steel. Based on the ultimate strength and ductility capacity, a ductility evaluation

method for thin-walled steel tubular columns is presented and discussed. The application of the method in ductility evaluation of steel tubular columns is demonstrated by comparing the computed strength and ductility of some cantilever columns with the test results.

2. Thin-walled Steel Box Columns

Steel columns in highway bridge systems are commonly composed of relatively thin-walled members of closed cross-sections, either box or circular in shape because of their high strength and torsional rigidity, see Figure 1a. Such structures are characterized by: failure attributed to local buckling in the thin-walled members; irregular distribution of the story mass and stiffness; strong beams and weak columns; and a need for the evaluation of residual displacement. These make the columns vulnerable to damage caused by the interaction of local and overall buckling in the event of a severe earthquake. The ductility behavior of steel tubular columns of welded box sections is mainly governed by local component members such as plates, with or without stiffeners.

The most important parameters considered in the practical design and ductility evaluation of thin-walled steel hollow box sections are the width-to-thickness ratio of the flange plate R_f for a box section, the radius-to-thickness ratio of the circular section R_t, and the slenderness ratio of the column $\bar{\lambda}$. While R_f and R_t influence local buckling of the section, $\bar{\lambda}$ controls the global stability. They are given by:

$$R_f = \frac{b}{t}\frac{1}{n\pi}\sqrt{3(1-\nu^2)\frac{\sigma_y}{E}} \quad \text{(for box section)} \tag{1}$$

$$R_t = \frac{r}{t}\sqrt{3(1-\nu^2)}\,\frac{\sigma_y}{E} \quad \text{(for circular section)} \tag{2}$$

$$\bar{\lambda} = \frac{2h}{r_g}\frac{1}{\pi}\sqrt{\frac{\sigma_y}{E}} \tag{3}$$

in which, $b =$ flange width; $t =$ plate thickness; $\sigma_y =$ yield stress; $E =$ Young's modulus; $\nu =$ Poisson's ratio; $n =$ number of subpanels divided by longtudinal stiffeners in each plate panel ($n = 1$ for unstiffened sections, see Figure 2d); $r =$ radius of the circular section; $h =$ column height; $r_g =$ radius of gyration of the cross section. In addition, the stiffener's slenderness ratio $\bar{\lambda}_s$, type of stiffener material, and magnitude of axial load P/P_y, are other important parameters considered in a practical design. The parameter $\bar{\lambda}_s$ controls the deformation capacity of the stiffeners and local buckling mode, and is given by:

$$\bar{\lambda}_s = \frac{1}{\sqrt{Q}} \frac{l_d}{r_s} \frac{1}{\pi} \sqrt{\frac{\sigma_y}{E}} \tag{4}$$

$$Q = \frac{1}{2R_f} [\beta - \sqrt{\beta^2 - 4R_f}] \leq 1.0 \tag{5}$$

$$\beta = 1.33R_f + 0.868 \tag{6}$$

where $r_s =$ radius of gyration of a T-shape cross-section consisting of one longitudinal stiffener and the adjacent subpanel of width (b/n) (see Figure 2d); $l_d =$ distance between two adjacent diaphragms (see Figure 2a); and $Q =$ local buckling strength of the sub-panel plate (Usami 1996). An alternative parameter reflecting the characteristics of the stiffener plate is the stiffener's relative flexural rigidity, γ, which is interdependent on $\bar{\lambda}_s$ and obtained from elastic buckling theory, DIN-4114 (1953). Thus only $\bar{\lambda}_s$ is considered in the ductility equations.

The elastic strength and deformation capacity of the column are expressed by the yield strength H_{y0}, and the yield deformation (neglecting shear deformations) δ_{y0}, respectively, corresponding to zero axial load. They are given by:

$$H_{y0} = \frac{M_y}{h} \tag{7}$$

$$\delta_{y0} = \frac{H_{y0} h^3}{3EI} \tag{8}$$

where $M_y =$ yield moment and $I =$ moment of inertia of the cross section. Under the combined action of buckling under constant axial and monotonically increasing lateral loads, the yield strength is reduced from H_{y0} to a value denoted by H_y. The corresponding yield deformation is denoted by δ_y. The value H_y is the minimum of yield, local buckling, and instability loads derived by the following equations:

$$\frac{P}{P_u} + \frac{0.85 H_y h}{M_y (1 - P/P_E)} = 1 \tag{9}$$

$$\frac{P}{P_u}+\frac{H_y h}{M_y}=1 \tag{10}$$

in which $P=$ the axial load; $P_y=$ the yield load; $P_u=$ the ultimate load; and $P_E=$ the Euler load. In the following section, a seismic performance evaluation method and an analytical procedure for determining ultimate strength and ductility capacity of thin-walled steel tubular columns are presented.

3. Ultimate Strength and Ductility Evaluation Method

The failure of a box steel column occurs when a displacement corresponding to the maximum strength (δ_m) or 95 percent strength after the peak (δ_{95}) is reached. Therefore the ductility of steel columns is defined by the index δ_m/δ_y, where δ_m is the displacement at the maximum strength (load) H_m, and δ_y is the yield displacement. Another ductility parameter is the ratio δ_{95}/δ_y, where δ_{95} is the displacement at 95% of H_m ($=H_{95}$) beyond the peak. These parameters are

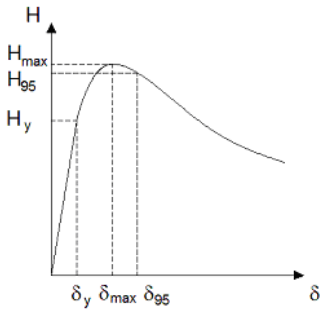

Figure 3. Definition of Strength and Ductility Factors

depicted schematically on the load-displacement curve in Figure 3. The parameter δ_{95}/δ_y is considered to be more suitable since it includes the effects of cyclic characteristics and takes advantage of the strength of steel at large plastic deformations. Also considering that the strength of thin-walled steel columns deteriorates significantly after the peak due to local buckling and cracks may occur near the column base after a large drop of strength owing to the low cycle fatigue of columns with small slenderness ratios, the adoption of 95% of peak is considered to be adequate.

4. Numerical Analysis

4.1 Analytical Model

Cantilever steel columns with box or circular cross-sections subjected to a constant axial force and cyclic lateral loadings are accounted for in the present analysis. The test specimens available in the literature are numerically analyzed following an elastoplastic large-displacement finite-element analysis procedure. For such thin-walled steel columns, local buckling always occurs

near the base of the columns. Therefore, the beam-column element is employed for the upper part of the column; while the shell element that accounts for the effect of local buckling is employed for the lower part of the column, see Figure 2b. The interface between the shell elements and the beam-column element is modeled using rigid beams, Figure 2b.

The column is stiffened by both longitudinal stiffeners and diaphragms, see Figures 1c and 2d. Only one-half of the columns is modeled because of the symmetry of the section and loading within the plane of the test, see Figures 2b and 5. The longitudinal stiffeners and each subpanel between longitudinal stiffeners are modeled by using a four-node doubly curved shell element (S4R) available in a general purpose finite element program *ABAQUS* (2005). The diaphragm is also modeled using the same type of shell element. Shell elements are used only up to the height of the third diaphragm, see Figures 2b and 5. The length between the base and the first diaphragm is divided into 18 segments, while the subsequent same lengths are divided into 9 segments along the column length. In the width and depth directions 24 elements are used. Each subpanel consists of eight columns of shell elements. Five columns of shell elements are assigned for longitudinal stiffeners, see Figures 2b and 5. For shell elements five layers are assumed across the thickness, and the spread of the plasticity is considered both through the thickness and along the element plane. The portion of the column beyond the third diaphragm is modeled using a beam-column element (B31), also included in the ABAQUS program. The sectional dimension of this element is chosen in such a way that the moment of inertia and the cross-sectional area of the element section are identical to those of one-half of the actual section. Ten beam-column elements are adopted to model the upper part of the specimen. The above-stated mesh divisions are determined by trial and error. It is found that such mesh divisions can give accurate results (Mamaghani 1996).

To investigate the effect of different material models on the failure strength and ductility of the column, three classical steel material models; IH, KH, and EPP material models, which are available in the ABAQUS software library are used with the Von Mises yield criterion. The residual stresses due to welding and the initial deflections of the flange and web plates are not considered in the analysis because their effect is insignificant on the cyclic behavior (Mamaghani 1996, Banno et al. 1998).

4.2 Box Columns of Stiffened Rectangular Sections

The accuracy of the cyclic elastoplastic large-displacement finite-element analysis procedure has been verified by the experimental data. Here, as an example, analysis of specimen B14 tested under constant axial load and lateral cyclic load by the Public Works Research Institute of Japan (Nishikawa et al. 1996) is presented. The dimensions and material properties for the specimen B14 are shown in Table 1. Where h, b, t, b_s, t_s are shown in Fig. 2; σ_y and σ_u are the yield stress and ultimate stress of the steel, respectively; H_y and δ_y are the lateral yield load and yield

Table 1. Geometric and Material Properties of the Columns B14

	h (mm)	b (mm)	t (mm)	b_s (mm)	t_s (mm)	P/P_y	σ_y (MPa)	σ_u (MPa)	H_y (kN)	δ_y (mm)
B14	3403	882	9	80	6	0.125	379	627	1017	13.8

displacement of the column, respectively; P_y is the yield load and P is the axial load on the column.

Analytical modeling of the specimen is shown in Figure 2. The specimen is a cantilever column modeling a bridge pier and is subjected to a constant axial load of P/P_y = 0.125 and cyclic lateral displacements of increasing amplitude $\pm\delta_y, \pm 2\delta_y, \ldots, \pm 8\delta_y$ at the column top. It has a stiffened square box section of size b = 882 *mm*, height of h = 3,403 *mm*, two equally spaced longitudinal stiffeners of 80×6 *mm*, and consists of five panels between equally spaced 6 *mm* plate diaphragms, see Figure 2a. The specimen's material is JIS SS400 mild steel (equivalent to ASTM A36) with the following material properties: yield stress σ_y = 379 MPa; ultimate tensile stress σ_u = 627 MPa; Young's modulus E = 206 GPa; strain at the onset of strain hardening ε_{st} = $14\varepsilon_y$; and Poisson's ratio ν = 0.3. The column's parameters are: R_f = 0.56 and $\bar{\lambda}_s$ = 0.63.

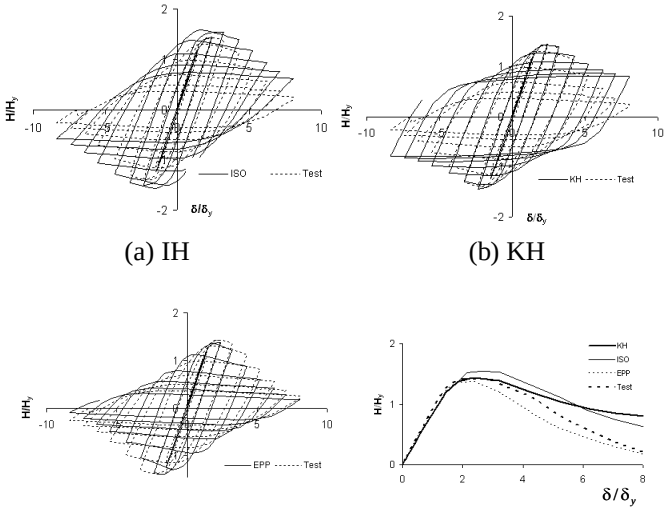

(a) IH (b) KH

(c) EPP (d) Envelope Curves

Figure 4. Comparisons of Predicted Hysteretic Curves and Test for the Column B14

Numerical and test results of normalized lateral load (H/H_y)-lateral displacement (δ/δ_y) hysteretic curves for the IH, KH, and EPP material models are plotted in Figures 4a, 4b, and 4c, respectively. The envelope curves of the positive (i.e. laterally pushed) side of the hysteretic curves are plotted in Figure 4d. The comparison reveals that the predicted hysteretic behavior, ultimate strength and ductility have good agreement with the test results. The initial stiffness of predicted curves agrees well with that of the test results for all three material models. The prediction by the EPP material model resulted in smaller strength values as compared to that of the test result, especially for the first five cycles. This is because the EPP model does not consider the strain-hardening effect of steel, which causes a decrease in strength of the column before buckling. However, the EPP material model predicts the post-buckling behavior of the column quite well, see Figure 4c. The shape of hysteretic loops predicted by the IH material model becomes quite wide near the peak-load because of the increase in elastic range due to cyclic loading. After buckling of the component plates of the column, cyclic behavior prediction is better because the buckling mode governs the behavior. In the case of the KH model, the prediction of hysteretic loops shows relatively good agreement with experimental results for the

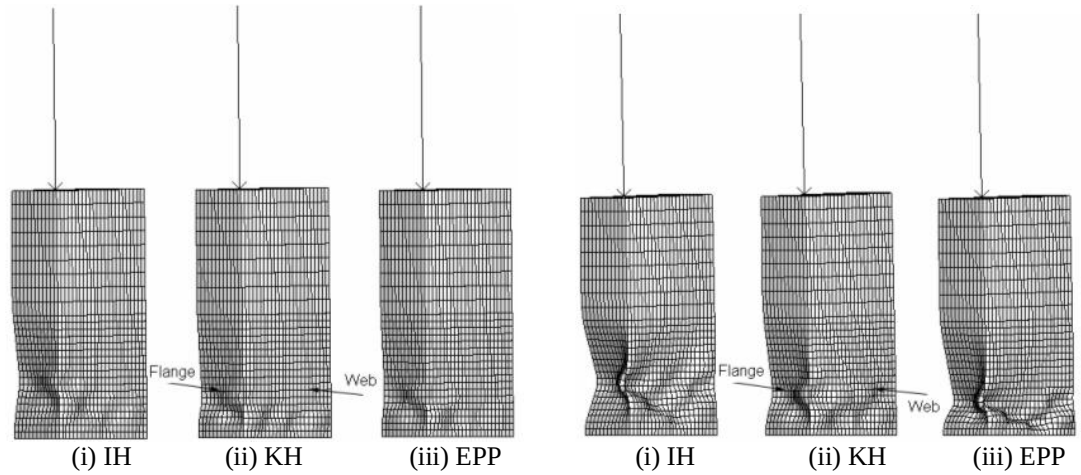

(i) IH (ii) KH (iii) EPP (i) IH (ii) KH (iii) EPP

(a) After the 4th cycle (b) At the end of loading after 8th cycle

Figure 5. Deformed Shape of the Column B14

first four cycles, see Figure 4b. The analytical results at the post-buckling stage overestimate the strength of the column. The strength and ductility ratio of test and analysis results are given in Table 2. If δ_{95}/δ_y ratio is considered a failure of the structure, the IH and KH material models predict the hysteretic loops well in this range. However, buckling of the component plates causes a large deterioration in post-buckling strength as seen from the lateral load-deflection curves, Figure 4. Both material models can be used for ductility evaluation of the thin-walled structures due to their reliable prediction of the behavior within the range of δ_{95}/δ_y.

Table 2. Strength and Ductility Ratio of the Column B14

Specimen		H_{max}/H_y	H_{95}/H_y	δ_{max}/δ_y	δ_{95}/δ_y
B14	Test	1.518	1.442	2.55	3.1
	ISO	1.455	1.383	2.48	3.38
	KH	1.383	1.314	2.27	3.26
	EPP	1.321	1.255	2.21	2.67

Deformation of the specimen after the 4th cycle and the final stage of analysis (8th cycle) are shown in Figures 5a and 5b, respectively. These results indicate that pronounced yielding and local buckling occur in the flange and web panel plates near the base of the column in the vicinity of the maximum load after eight cycles, $\delta/\delta_y = \pm 4$. The buckling pattern of the flange and web panel plates is simulated well. These results verify the accuracy of the above-discussed analytical procedure in predicting the cyclic elastoplastic behavior of thin-walled steel tubular columns.

The predicted results given in Table 2 (δ_{95}/δ_y = 3.1 for test and δ_{95}/δ_y =3.26 for KH model) suggests that the deformation corresponding to 95% of the maximum strength after peak from

Table 3. Geometric and Material Properties of the Columns P1

	h (mm)	D (mm)	t (mm)	P/P_y	σ_y (MPa)	σ_u (MPa)	H_y (kN)	δ_y (mm)
P1	3403	891	9	0.12	289.6	510	415.2	10.6

cyclic analysis employing the ABAQUS/KH can be used to verify the validity of the proposed ductility evaluation method.

4.3 Tubular Columns of Circular Sections

The analysis of a cantilever steel column with a circular cross-section subjected to a constant axial force and cyclic lateral loadings is presented in this section. The test was conducted by the Public Works Research Institute of Japan (Nishikawa et al. 1996). The specimen dimensions and material properties are given in Table 3. The finite element model is shown in Figure 2b. The column is divided into two parts similar to the stiffened box column discussed above. The length from the base that equals the radius of the column is divided into 15 segments, while the adjacent length of three times of the radius is divided into 10 segments along the column length. In the circumferential direction, 30 shell elements are used, see Figures 2b and 7a. Beam-column element, B21, having a circular section, is used for the upper part. A stiff plate with infinite bending stiffness is used in the interface between the beam-column element and shell-elements.

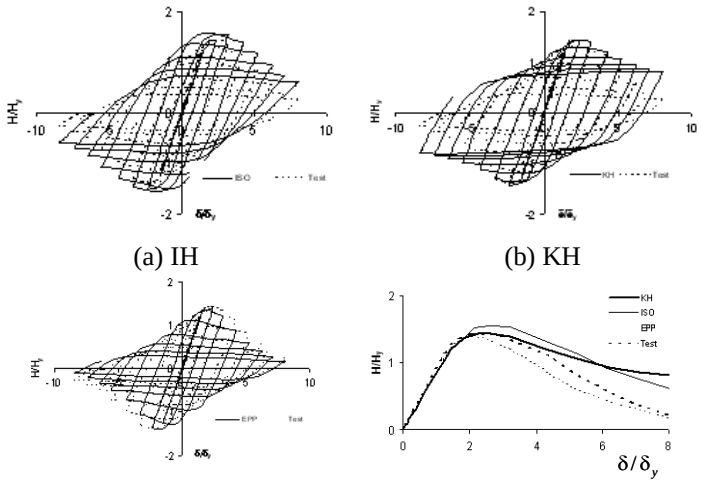

(a) IH (b) KH

(c) EPP Material Models (d) Envelope Curves

Figure 6. Comparisons of Predicted Hysteretic Curves and Test for the Column P1

Figures 6a, 6b, and 6c, respectively, show a comparison of test results with the analytical results for the IH, KH and EPP material models. Similar to the stiffened box column referred to above, the EPP model gives smaller strength values because this model does not consider the strain hardening of steel. The shape of the hysteretic loops predicted by the IH model becomes quite wide near the peak because of the increase in the elastic range. In addition, the IH material model overestimates the strength for all cycles. In the case of the KH model, the prediction of hysteretic loops for the first cycles shows good agreement with experimental results due to its constant

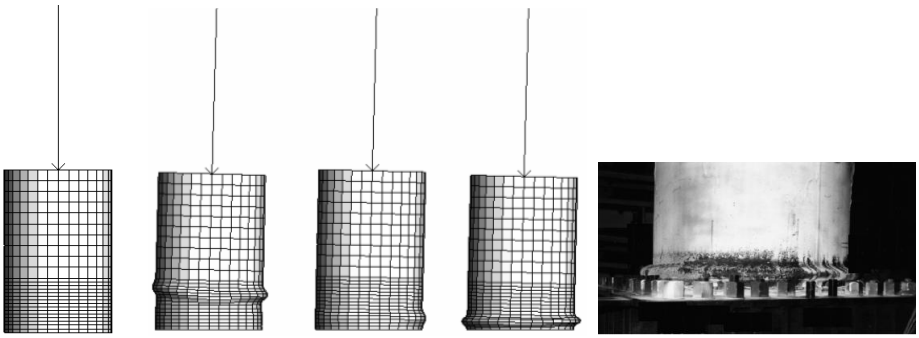

Figure 7. Initial Configuration and Deformed Shape of the Column B14 At the End of Cyclic Loading: (a) Analysis, (b) Test (Nishikawa et al. 1996)

elastic range. On the other hand, the analytical results at the post-buckling stage have been overestimated because in the test the elastic range of the material decreased with an increase in cyclic load (Bauschinger effect), whereas the KH model assumes a constant elastic range for the material. However, the failure point, $\delta_{95}/\delta_{y,}$ stays within the range of well-predicted loops, as was the case for the rectangular box columns. The strength and ductility ratio of test and analysis results are given in Table 4. Envelope curves of the test and analysis results are plotted in Figure 6d. The KH material model closely predicts the ultimate strength and ductility values as shown in Table 4. The deformation of the test specimen at the final stage of loading is shown in Figures 7a and 7b, obtained from the analysis and test, respectively. The EPP material model predicts the local buckling behavior quite well as shown in Figure 7.

Table 4. Strength and Ductility Ratio of the Column P1

Specimen		H_{max}/H_y	H_{95}/H_y	δ_{max}/δ_y	δ_{95}/δ_y
P1	Test	1.42	1.35	2.42	3.12
	ISO	1.55	1.47	2.6	3.55
	KH	1.44	1.36	2.41	3.34
	EPP	1.37	1.3	2.31	2.72

5. Conclusions

This paper dealt with the cyclic behavior and ductility evaluation of thin-walled stiffened steel box columns subjected to cyclic lateral loading in the presence of constant axial load. The basic characteristics of steel box columns were noted. The results of finite-element analyses employing the kinematic hardening, isotropic hardening, and elastic perfectly plastic material models on the cyclic elastoplastic behavior of steel box columns were presented. A method for evaluating ultimate strength and ductility of box columns was presented. The application of the method was verified by comparing the computed strength and ductility of some cantilever columns with the test results. It is concluded that the ABAQUS program employing the kinematic hardening

material model can be used to predict the ultimate strength and ductility of steel tubular columns with reasonable accuracy.

References

ANSYS *(*2008). *User's manual*, *Version 11,* ANSYS Structural Analysis Guide, ANSYS Inc.

Banno, S., I. H.P. Mamaghani, T. Usami, E. Mizuno, 1998. Cyclic elastoplastic large deflection analysis of thin steel plates. *Journal of Engineering Mechanics, ASCE*, 124(4), 363-370.

DIN-4114. (1953), "Stahbau, Stabilitatsfalle (Knickung, Kippung, Beulung)", Berechnungsgrund-lagen, Richtlinien, Blatt2. Berlin, Germany, (in German).

Fukumoto, Y. (2004), "Cyclic Performance Assessment of Stiffened Box Columns with Thickness Tapered Plates", SSRC 2004 Beedle Award Paper, Long Beach, California, PP. 1-18.

Gao, S. B., Usami, T., and Ge, H. B. (1998). ''Ductility Evaluation of Steel Bridge Piers with Pipe Sections.'' *J. Engrg. Mech., ASCE,* 124(3), pp.260–267.

Hajjar, J.F. (2000), "Concrete-filled Steel Tube Columns Under Earthquake Loads", Progress in Structural Engineering and Materials, Vol. 2(1), pp. 72–82.

Japanese Road Association (JRA). (1996). "Specification for Highway Bridges", Part V, Tokyo (in Japanese).

Kitada, T., Nakai, H., Matsumura, M. and Kagayama, T. (2000), "Experimental Study on Seismic Retrofitting Method of Stiffened Plates in Existing Steel Bridge Piers Under Cyclic Loading", *Journal of Structural Engineering, JSCE,* Vol. 46, pp. 127–134 (in Japanese).

Mamaghani, I.H.P. (2008). Seismic Design and Ductility Evaluation of Thin-Walled Steel Bridge Piers of Box Sections, *Journal of the Transportation Research Board*, No. 2050, Washington D.C., pp. 137-142.

Mamaghani, I.H.P. (1996), "Cyclic Elastoplastic Behavior of Steel Structures: Theory and Experiments", *Doctoral Dissertation,* Department of Civil Engineering, Nagoya University, Nagoya, Japan.

Mamaghani, I.H.P. and Packer J.A. (2002), "Inelastic Behavior of Partially Concrete-Filled Steel Hollow Sections", *4th Structural Specialty Conference*, The Canadian Society for Civil Engineering, Montréal, Québec, Canada, pp. s71:1-10.

Mamaghani, I.H.P., Shen, C., Mizuno, E. and Usami, T. (1995), "Cyclic Behavior of Structural Steels, I: Experiments", *Journal of Engineering Mechanics, ASCE,* USA, Vol.121, No.11, pp. 1158-1164.

Mamaghani, I.H.P., Usami, T. and Mizuno, E. (1996), "Cyclic Elastoplastic Large Displacement Behaviour of Steel Compression Members", *Journal of Structural Engineering, JSCE,* Japan, Vol. 42A, pp. 135-145.

Mamaghani, I.H.P., Usami, T. and Mizuno, E. (1996), "Inelastic Large Deflection Analysis of Structural Steel Members Under Cyclic Loading", *Engineering Structures,* UK, Elsevier Science, Vol. 18(9), pp. 659-668.

Mamaghani, I.H.P., Usami, T. and Mizuno, E. (1997), "Hysteretic Behavior of Compact Steel Box Beam-Columns", *Journal of Structural Engineering, JSCE,* Vol. 43A, pp. 187-194.

Nakanishi, K., Kitada, T. and Nakai, H. (1999), "Experimental Study on Ultimate Strength and Ductility of Concrete Filled Steel Columns Under Strong Earthquake", *Journal of Constructional Steel Research,* No. 51, pp. 297–319.

Nishikawa, K., Yamamoto, S., Natori, T., Terao, K., Yasunami, H. and Terada, M. (1998), "Retrofitting for Seismic Upgrading of Steel Bridge Columns", *Engineering Structures,* Vol. 20, Nos. 4~6, pp. 540-551.

Nishikawa K, Yamamoto S, Natori T, Terao K, Yasunami H, Terada M. (1996). "An experimental study on improvement of seismic performance of existing steel bridge piers." *J. of Struct. Engrg., JSCE* 1996; 42A, 975-986 (in Japanese).

Shen, C., Mamaghani, I.H.P., Mizuno, E. and Usami, T. (1995), "Cyclic Behavior of Structural Steels, II: Theory", *Journal of Engineering Mechanics, ASCE,* USA, Vol.121, No.11,1165-1172.

Uenoya, M., Nakamura, M., Fukumoto, Y., Yamamoto, S. (2003), "Cyclic Performance of Square Box Columns with Thickness Tapered Plates", *J. of Structural Engineering, JSCE,* Vol. 49A, pp. 115-125 (in Japanese).

Usami, T. (1996), "Interim Guidelines and New Technologies for Seismic Design of Steel Structures", Committee on New Technology for Steel Structures, JSCE, Tokyo (in Japanese).

Usami, T., Suzuki, M., Mamaghani, I.H.P. and Ge, H.B. (1995), "A Proposal for Check of Ultimate Earthquake Resistance of Partially Concrete Filled Steel Bridge Piers", *Journal of Structural Mechanics and Earthquake Engineering, JSCE,* Tokyo, 525/I-33, 69-82, (in Japanese).